Russian Journal of General Chemistry, Vol. 72, No. 5, 2002, pp. 717–728. Translated from Zhurnal Obshchei Khimii, Vol. 72, No. 5, 2002, pp. 769–781.

Isomerism and Vibration Spectra of M_2XO_4 Molecules (M = Li, Na, K; X = S, Se, Te, Cr, Mo, W)

V. G. Solomonik and A. V. Marenich

Ivanovo State University of Chemical Engineering, Ivanovo, Russia

Received June 19, 2000

Abstract — The equilibrium geometries, isomerization energies, force fields, vibration frequencies, and band intensities in the IR spectra of M_2XO_4 molecules (M = Li, Na, K; X = S, Se, Te, Cr, Mo, W) were calculated *ab initio* by the Hartree–Fock method in extended basis sets using relativistic effective core potentials. The relative energies of alternative structures were refined by the configuration interaction method taking into account single- and double-excited configurations, with the Davidson correction for quartic excitations. The results show that the chemical bonds between the metal atom and the acid residue XO_4 are highly polar. The majority of M_2XO_4 molecules have two isomers. In both isomers the XO_4^{2-} anion coordinates the metal cations M^+ in the bisbidentate (*bb*) fashion. The equilibrium configurations of the nuclei in the ground (*bb*) and excited (*bb*') isomers have the D_{2d} and C_s symmetry, respectively. In the *bb* isomer, the cations coordinate at the opposite, and in the *bb*' isomer, at the adjacent edges of the XO_4^{2-} anion, having the shape of a distorted tetrahedron. The relative energy of the *bb*' isomer is 9–28 kJ mol^{-1}. The energy barriers to intramolecular rearrangements *bb*'(C_s) → *bb*(D_{2d}) are also low: 15–35 kJ mol^{-1}. These results show that the M_2XO_4 molecules are structurally nonrigid, with a "polytopic" character of the M–XO_4 chemical bonds. The calculation results were compared to the published experimental data on the structure and vibration spectra of the M_2XO_4 molecules.

Molecules of alkali metal sulfates, selenates, chromates, molybdates, and tungstates M_2XO_4 have been studied by gas-phase electron diffraction [1–4] and by Raman and IR spectroscopy using the matrix isolation technique [5–10]. The structural information derived from these studies is far from being unambiguous and exhaustive. All the experimental data were interpreted assuming a single type of equilibrium configurations of nuclei in M_2XO_4 molecules: configurations of the D_{2d} symmetry in which the M^+ cations coordinate with two opposite O–O edges of a distorted XO_4^{2-} tetrahedron (Fig. 1a). In a spectroscopic study of M_2SO_4 molecules [5], bistridentate (*tt*) coordination of M^+ ions with the SO_4^{2-} anion (Fig. 1d) was considered along with the bisbidentate (*bb*) coordination, but in interpretation of the experimental results the bisbidentate (D_{2d}) structure was preferred. The possible isomerism of the other M_2XO_4 molecules was discussed in none of the previous papers. As for theoretical studies, only the molecules of lithium, sodium, and potassium sulfates were investigated (see [11, 12] and references therein). No quantum-chemical calculations were performed for the other M_2XO_4 molecules.

Here we report on the first systematic *ab initio* study of M_2XO_4 salt molecules (M = Li, Na, K; X = S, Se, Te, Cr, Mo, W). We have determined their geometries, revealed specific features of their force fields and vibration spectra, and found regular trends in variation of molecular parameters on replacement of X and M atoms by their heavier analogs (X: S → Se → Te, Cr → Mo → W; μ: Li → Na → K) with the

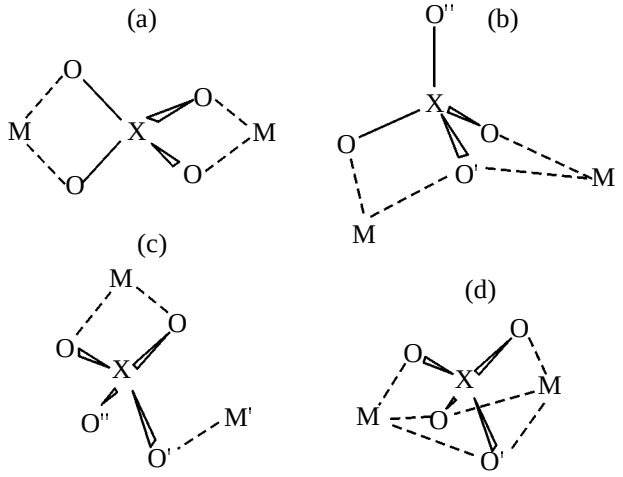

Fig. 1. Alternative configurations of M_2XO_4 molecules: (a) bisbidentate (*bb*), D_{2d} symmetry; (b) bisbidentate (*bb*'), C_s symmetry; (c) monobidentate (*mb*), C_1 symmetry; and (d) bistridentate (*tt*), C_{2v} symmetry.

1070-3632/02/7205-0717 $27.00

aim to predict the structure and spectra of heavier M_2XO_4 molecules (M = Rb, Cs). The properties of the XO_4 fragment in the M_2XO_4 molecule were compared to those of the free XO_4^{2-} ion [13]. The minimum-energy pathways of isomerization of M_2XO_4 molecules were studied. The structure and vibration spectra of the molecules of lithium, sodium, and potassium tungstates were studied by us *ab initio* previously [14]; some of those results are used in this work.

Calculation details. Calculations were performed using the GAMESS program [15]. The following basis sets of grouped Gaussian functions were used: Li, (9*s*3*p*1*d*)/[4*s*3*p*1*d*]; Na, (12*s*8*p*1*d*)/[6*s*4*p*1*d*]; K, (14*s*11*p*3*d*)/[9*s*8*p*3*d*]; for alkali metal sulfates, also O, (9*s*5*p*1*d*)/[4*s*2*p*1*d*]; S, (12*s*9*p*1*d*)/[6*s*4*p*1*d*]. These basis sets are described in detail in [12]. In calculations of M_2XO_4 molecules with X = Se, Te, Cr, Mo, and W, we used the effective core potentials by Stevens *et al*. for the Se, Te, Cr, Mo, W, and O atoms [16, 17] (for X atoms the potentials are relativistic). The valence orbitals of the oxygen atom were described by the 31G basis [16] supplemented by the polarization *d* function with an exponent of 0.8. The basis sets of type 41G for the Se and Te atoms [17] were supplemented by two polarization *d* functions [18] with exponents of 0.489 and 0.144 for Se, and 0.305 and 0.096 for Te. The valence orbitals of the Cr, Mo, and W atoms were described by the following basis sets [17]: Cr, (8*s*8*p*6*d*)/[4*s*4*p*3*d*]; Mo, (8*s*8*p*5*d*)/[4*s*4*p*3*d*]; and W, (7*s*7*p*5*d*)/[4*s*4*p*3*d*].

The equilibrium geometries of the M_2XO_4 molecules were optimized, and their vibrational spectra and minimum-energy pathways of intramolecular rearrangements calculated, by the Hartree–Fock (HF) method. The relative energies of alternative configurations were optimized by the method of configuration interactions taking into account single- and double-excited configurations with a Davidson correction [19] for quartic excitations (CISD+Q). The CISD+Q calculations were performed for the geometries optimized on the HF level. When constructing the wave function of the CISD method, we did not take into account only the electron excitations from the molecular orbitals corresponding to the 1*s* orbitals of O and Na and to the 1*s*, 2*s*, and 2*p* orbitals of S and K. The resulting wave functions consisted of the following numbers of configurations (within the D_2 symmetry): 398306 (Li_2SO_4), 374581 (Li_2SeO_4, Li_2TeO_4), 681583 (Li_2CrO_4, Li_2MoO_4, Li_2WO_4), 736291 (Na_2SO_4), 693253 (Na_2SeO_4, Na_2TeO_4), 1145341 (Na_2CrO_4, Na_2MoO_4, Na_2WO_4), 1558495 (K_2SO_4), 1495585 (K_2SeO_4, K_2TeO_4), and 2327403 (K_2CrO_4, K_2MoO_4, K_2WO_4).

The geometries of the M_2XO_4 molecules were optimized using the analytically calculated gradients. Calculations of the force constants and dipole moment derivatives with respect to normal coordinates were performed by a numerical method using the procedures and software described in [20].

Structure of M_2XO_4 molecules. For each molecule we considered several configurations of nuclei, corresponding to different types of coordination of M^+ cations with tetrahedral anions XO_4^{2-} (Fig. 1). The optimized geometries, dipole moments, and relative energies of the alternative structures, calculated in the HF approximation, are listed in Tables 1 and 2. Calculations show that the ground equilibrium configuration of all the molecules under consideration is the *bb* structure of the D_{2d} symmetry (Fig. 1a), corresponding to the bisbidentate coordination of two M^+ cations with the XO_4^{2-} anion. The bisbidentate structures *bb*' of the C_s symmetry in which the cations are coordinated at the adjacent O–O edges of the XO_4^{2-} tetrahedron (Fig. 1b) correspond to local minima on the potential energy surfaces of all the molecules except K_2SO_4, in which this structure corresponds to the first-order saddle point. Presumably, in Rb_2SO_4 and Cs_2SO_4 the *bb*' structures also correspond to the saddle points on the potential energy surfaces.

Calculations show that the relative energy $h(bb') = E(bb') - E(bb)$ of the C_s structures in the series $Li_2XO_4 \rightarrow Na_2XO_4 \rightarrow K_2XO_4$ varies only slightly and in most cases somewhat increases. If this trend keeps in going to Rb and Cs, for Rb_2XO_4 and Cs_2XO_4 the relative energy $h(bb')$ will be within 20–30 kJ mol^{-1}. It is interesting that the trends in variation of $h(bb')$ in the series $M_2SO_4 \rightarrow M_2SeO_4 \rightarrow M_2TeO_4$ and $M_2CrO_4 \rightarrow M_2MoO_4 \rightarrow M_2WO_4$ are opposite: Whereas in the first case $h(bb')$ decreases by 3–10 kJ mol^{-1}, in the second case it increases by 11–14 kJ mol^{-1}.

The results of calculating the minimum-energy pathways of the intramolecular rearrangement $bb'(C_s) \rightarrow bb(D_{2d})$ in the Li_2SO_4 and K_2WO_4 molecules are shown in Fig. 2. Calculations show that the peaks of the activation barriers of this rearrangement correspond to the monobidentate (*mb*) structures of the C_1 symmetry (Fig. 1a). The height $h(mb) = E(mb) - E(bb')$ of the barrier separating the local $[bb'(C_s)]$ and global $[bb(D_{2d})]$ minima on the potential energy surface is 35 kJ mol^{-1} for Li_2SO_4 and 12 kJ mol^{-1} for K_2WO_4. It should be noted that the heights of the activation barriers $h(mb)$ noticeably exceed the vibrational quanta corresponding to the vibrational motion of nuclei in the *bb*' structures of the M_2XO_4 molecules directed along the most "nonrigid" normal coordinate determining the minimum-energy

Table 1. Properties of μ_2XO_4 molecules (X = S, Se, Te)[a]

Property	Li_2SO_4	Na_2SO_4	K_2SO_4	Li_2SeO_4	Na_2SeO_4	K_2SeO_4	Li_2TeO_4	Na_2TeO_4	K_2TeO_4
				bb(D_{2d}) structure					
R_e(MO)	1.855	2.199	2.523	1.883	2.230	2.559	1.906	2.259	2.595
R_e(XO)	1.475	1.476	1.476	1.618	1.617	1.617	1.799	1.797	1.796
α_e(OXO)	103.9	106.2	107.2	100.4	103.9	105.4	94.2	98.9	101.2
				bb'(C_s) structure					
R_e(XO'')	1.422	1.438	1.451	1.570	1.582	1.590	1.758	1.765	1.770
R_e(XO')	1.546	1.533	1.519	1.681	1.669	1.658	1.856	1.844	1.834
R_e(XO)	1.475	1.473	1.470	1.619	1.616	1.614	1.801	1.798	1.796
R_e(MO')	1.877	2.235	2.596	1.900	2.258	2.616	1.913	2.281	2.648
R_e(MO)	1.830	2.177	2.510	1.854	2.207	2.536	1.875	2.229	2.557
α_e(O'XO)	101.6	104.5	106.3	98.4	102.4	104.4	92.7	97.8	100.5
β_e(O''XO)	113.9	112.7	111.8	114.8	113.4	112.6	116.4	114.8	113.8
γ_e(O''XO')	111.7	109.5	107.9	113.8	110.6	109.0	117.8	113.7	111.7
θ_e[b]	167.4	158.8	147.1	169.2	162.1	155.2	171.8	167.4	163.6
μ_e	9.5	11.6	11.4	9.6	12.1	12.8	9.2	12.8	14.2
h(HF)	27	27	24	25	26	25	18	24	25
h(CISD+Q)	21	22	–	18	22	–	11	19	–
				tt(C_{2v}) structure					
R_e(XO)	1.453	1.456	1.459	1.580	1.601	1.604	1.763	1.775	1.786
R_e(XO')	1.492	1.495	1.493	1.668	1.635	1.632	1.857	1.827	1.808
R_e(MO)	2.016	2.307	2.601	2.671	2.408	2.672	3.073	2.914	2.785
R_e(MO')	2.207	2.475	2.794	1.986	2.523	2.866	1.961	2.413	2.944
α_e(OXO)	120.0	116.7	114.8	122.9	121.0	117.7	124.5	126.6	124.1
β_e(OXO')	108.4	109.1	109.3	109.6	108.4	108.9	110.5	108.3	107.8
μ_e	6.7	9.2	10.5	9.7	9.4	10.7	10.0	11.5	10.8
h(HF)	114	48	21	129	64	32	139	103	63
h(CISD+Q)	95	38	13	109	49	24	120	85	56

[a] The dimensions are as follows: internuclear distances R_e, Å; bond angles α_e, β_e, γ_e and dihedral angles θ_e, deg; dipole moments μ_e, D; relative energies $h(bb') = E(bb') - E(bb)$ and $h(tt) = E(tt) - E(bb)$, kJ mol^{-1}. [b] Dihedral angle between the XO_2 and O_2M planes in the XO_2M ring. The same for Table 2.

pathway of the rearrangement *bb*'(C_s) → *bb*(D_{2d}). The potential well of the *bb*'(C_s) structure accommodates 18 (Li_2SO_4) and 14 (K_2WO_4) vibrational energy levels calculated in the harmonic approximation. Hence, the C_s structures of the M_2XO_4 molecules can be experimentally detectable, e.g., at low temperatures using the matrix isolation technique. Nevertheless, very low values of the relative energies of the isomers and of the energy barriers of structural rearrangements of M_2XO_4 molecules indicate that these molecules are structurally nonrigid, with the "polytopic" character of chemical bonds between the M atoms and XO_4 fragment.

The bistridentate structures *tt* of the C_{2v} symmetry (Fig. 1d) correspond to the local minima on the potential energy surface of two molecules: K_2SO_4 and K_2CrO_4. The local (*tt*) and global (*bb*) minima on the potential energy surfaces of these molecules are separated by a very small energy barrier corresponding to the distorted bistridentate structure *tt*'(C_1): $h(tt') = E(tt') - E(tt)$ = 35 (K_2SO_4) or 2 (K_2CrO_4) cm^{-1}. So small $h(tt')$ does not allow the *tt*(C_{2v}) structures to be considered as existing isomers of the K_2SO_4 and K_2CrO_4 molecules. On the potential energy surfaces of the other M_2XO_4 molecules under consideration, the bistridentate structures *tt* of the C_{2v} symmetry correspond to the saddle points of the first (Li_2SeO_4, Li_2TeO_4, Li_2CrO_4, Li_2MoO_4, Li_2WO_4, Na_2TeO_4, K_2SeO_4), second (Li_2SO_4, Na_2SO_4, Na_2SeO_4, Na_2CrO_4, K_2TeO_4, K_2MoO_4, K_2WO_4), and third orders (Na_2MoO_4 and Na_2WO_4). The relative energy of the *tt* structures $h(tt) = E(tt) - E(bb)$ of the M_2XO_4 molecules appreciably (by 25–47 kJ mol^{-1}) decreases with decreasing weight of the central atom X (X = Te → Se → S, W → Mo → Cr).

The energies $h(tt)$ decrease in the series Li_2XO_4 →

Table 2. Properties of M_2XO_4 molecules (X = Cr, Mo, W)

Property	Li_2CrO_4	Na_2CrO_4	K_2CrO_4	Li_2MoO_4	Na_2MoO_4	K_2MoO_4	Li_2WO_4	Na_2WO_4	K_2WO_4
				bb(D_{2d}) structure					
R_e(MO)	1.858	2.223	2.538	1.898	2.264	2.586	1.910	2.270	2.592
R_e(XO)	1.604	1.605	1.605	1.753	1.754	1.754	1.763	1.763	1.763
α_e(OXO)	101.6	105.0	105.9	96.6	101.0	102.6	96.5	101.0	102.5
				bb'(C_s) structure					
R_e(XO'')	1.533	1.548	1.556	1.687	1.698	1.706	1.706	1.716	1.722
R_e(XO')	1.699	1.684	1.670	1.836	1.822	1.808	1.828	1.818	1.805
R_e(XO)	1.604	1.602	1.602	1.758	1.756	1.756	1.769	1.766	1.766
R_e(MO')	1.849	2.229	2.571	1.901	2.286	2.640	1.929	2.308	2.666
R_e(MO)	1.869	2.226	2.532	1.891	2.247	2.554	1.884	2.242	2.550
α_e(O'XO)	100.3	104.5	105.7	95.4	100.7	102.6	95.4	100.5	102.4
β_e(O''XO)	113.0	111.5	111.1	114.7	112.7	112.1	115.0	113.1	112.4
γ_e(O''XO')	112.9	110.0	109.3	115.6	112.2	110.9	114.8	111.7	110.6
θ_e	171.6	163.9	160.8	173.2	168.1	165.5	173.2	168.1	165.7
μ_e	8.5	11.3	12.6	8.8	12.2	13.8	9.2	12.6	14.2
h(HF)	11	12	17	18	20	23	26	26	28
h(CISD+Q)	9	10	–	16	17	–	23	24	–
				tt(C_{2v}) structure					
R_e(XO)	1.545	1.584	1.588	1.694	1.787	1.750	1.714	1.794	1.765
R_e(XO')	1.683	1.626	1.623	1.840	1.722	1.756	1.833	1.732	1.760
R_e(MO)	2.777	2.391	2.664	3.139	2.076	2.652	3.122	2.060	2.616
R_e(MO')	1.948	2.503	2.837	1.957	3.715	3.065	1.978	3.886	3.145
α_e(OXO)	116.2	119.1	116.7	115.0	114.5	120.8	117.2	113.5	121.1
β_e(OXO')	111.7	108.9	109.2	113.2	108.7	108.3	112.5	108.8	108.1
μ_e	9.1	9.4	10.7	9.9	1.5	10.0	10.6	0.7	9.5
h(HF)	115	49	33	144	88	64	159	85	68
h(CISD+Q)	104	36	28	136	88	59	147	91	60

$Na_2XO_4 \rightarrow K_2XO_4$, which suggests that for Rb_2XO_4 and Cs_2XO_4 the relative energies of the tt structures will be still lower. To estimate *h*(*tt*) for Rb_2XO_4 and Cs_2XO_4, we postulated the following relationship between *h*(*tt*) and the ionic radius of alkali metal $R = R(M^+)$:

$$h = a + b/R + c/R^2. \quad (1)$$

Extrapolation by formula (1) of the relative energies of the *tt* structures of M_2XO_4 (M = Li, Na, K), calculated in the CISD+Q approximation, was performed using the ionic radii evaluated in [21] from the internuclear distances in diatomic alkali metal halide molecules (Table 1, model 1 in [21]). The following values of *h*(*tt*) (kJ mol^{-1}) were obtained for Rb_2XO_4 and Cs_2XO_4:

X =	S	Se	Te	Cr	Mo	W
M = Rb	6	17	47	28	51	51
M = Cs	1	12	39	28	43	44

Hence, it can be expected that, similar to the molecules of M_2XO_4 salts of light alkali metals (M = Li, Na, K), the ground configuration of nuclei in the Rb_2XO_4 and Cs_2XO_4 molecules will be that of the D_{2d} symmetry. However, the nearly zero *h*(*tt*) values for the rubidium and cesium sulfate molecules show that in these molecules the cations virtually freely migrate around the SO_4^{2-} ion, i.e., the structural nonrigidity of these molecules is strongly pronounced. Estimations of *h*(*tt*) for the rubidium and cesium salts M_2SO_4 also show that in the sulfates and selenates the energy of the *tt* structures should be lower than that of the bis-bidentate *bb*' structures. It was interesting to check these assumptions by performing direct *ab initio* calculations of the Rb_2XO_4 and Cs_2XO_4 molecules.

The Mulliken population analysis of M_2XO_4 molecules shows that the charges on alkali metal atoms *q*(M) are close to unity, i.e., the chemical bonds between the XO_4 fragment and the metal atoms are essentially polar. The low equilibrium internuclear distances R_e(X–O) in the M_2XO_4 molecules are close

to R_e(X–O) in free XO_4^{2-} ions (T_d symmetry) [13]. The angles between the X–O bonds in the *bb*, *bb*', and tt structures, as a rule, somewhat differ from the ideal tetrahedral angle (109°28′): the mean deviation is 6°, and the largest deviation (17°) is observed for the α_e(OXO) bond angle in the *tt* structure of the Na_2TeO_4 molecule. Hence, the structure of the M_2XO_4 molecules can be approximately described by the model $(M^+)_2[XO_4]^{2-}$, in which the XO_4 fragment of the M_2XO_4 molecule is considered as an XO_4^{2-} anion electronically polarized and geometrically distorted in the field of two M^+ cations. The degree of polarization and deformation of the XO_4^{2-} ion decreases in going from lighter to heavier alkali metals M ($Li_2XO_4 \rightarrow Na_2XO_4 \rightarrow K_2XO_4$), which is due to a decrease in the polarizing power of the M^+ ion with an increase in its ionic radius. The degree and character of the polarization and deformation of the XO_4^{2-} ion noticeably change as the position of the cations relative to the anion is changed. In going from the *bb* structure to less symmetrical configurations, the XO_4^{2-} fragment becomes appreciably more distorted (Tables 1, 2). The equilibrium internuclear distances R_e(X–O) noticeably increase in the series $M_2SO_4 \rightarrow M_2SeO_4 \rightarrow M_2TeO_4$ (for the D_{2d} structures, by 0.14 Å in going from S to Se and by 0.18 Å in going from Se to Te). In the series $M_2CrO_4 \rightarrow M_2MoO_4 \rightarrow M_2WO_4$, the pattern is somewhat different: in going from chromates to molybdates R_e(X–O) increases by 0.15 Å, whereas in going from molybdates to tungstates it increases by only 0.01 Å, which is due to lanthanide contraction.

The results of our calculations demonstrate essential similarity in the structures of alkali metal salts with oxyanions of Group VI elements, both *d* [$M_2X^{(d)}O_4$, $X^{(d)}$ = Cr, Mo, W] and *p* [$M_2X^{(p)}O_4$, $X^{(p)}$ = S, Se, Te]. The parameters of the M_2CrO_4 molecules are closer to those of the M_2SeO_4 molecules, and the parameters of the M_2MoO_4 and M_2WO_4 molecules, to those of the M_2TeO_4 molecules.

To assess how consideration of the electron correlation affects the results of calculations of the structures and vibration spectra of M_2XO_4 molecules, we have performed complete optimization of geometry by the CISD and CISD+Q methods for the ground isomer *bb*(D_{2d}) and by the CISD method, for the excited isomer *bb*'(C_s) of the Li_2SO_4 molecule. In the optimization in the CISD approximation, we used the analytical gradients. The equilibrium geometries of the ground isomer of the molecule, calculated in the CISD+Q and CISD (in parentheses) approximations, are as follows: R_e(Li–O) 1.863 (1.858), R_e(S–O) 1.503 (1.490) Å, α_e(OSO) 104.3° (104.2°). The geometries of the *bb*'(C_s) isomer calculated by the CISD method are as follows: R_e(S–O'') 1.435, R_e(S–O') 1.568, R_e(S–O) 1.490, R_e(Li–O') 1.871, R_e(Li–O) 1.836 Å, α_e(O'SO) 101.6°, β_e(O''SO) 114.0°, γ_e(O''SO') 111.5°, and θ_e 166.9°. Thus, taking into account the electron correlation in the computations increases the calculated internuclear distances R_e(S–O) in the ground and excited isomers of the Li_2SO_4 molecule by 0.012–0.028 Å, whereas the R_e(Li–O) distances change by no more than 0.008 Å. The α_e, β_e, γ_e, and θ_e angles change by no more than 0.5° when the electron correlation is taken into account. Similar correlation corrections to the molecular geometries can be also expected for the other M_2XO_4 molecules. The force constant matrices calculated by the CISD and CISD+Q methods confirmed the conclusion, following from the Hartree–Fock calculations, that the Li_2SO_4 molecule can exist in the form of two isomers with the D_{2d} and C_s symmetry. The relative energy h(bb') calculated in the CISD and CISD+Q approximations using the geometries of the *bb*(D_{2d}) and *bb*'(C_s) structures optimized in the CISD approximation amounted to 22.8 (CISD) and 20.6 kJ mol^{-1} (CISD+Q). This values differ, respectively, by only 0.2 and 0.5 kJ mol^{-1} from the *h*(*bb*') values calculated using the HF-optimized geometries: *h*(CISD) 23.0 and *h*(CISD+Q) 21.1 kJ mol^{-1}. This result suggests that for the relative energies of the *bb*' configurations of the other M_2XO_4 molecules the error originating from

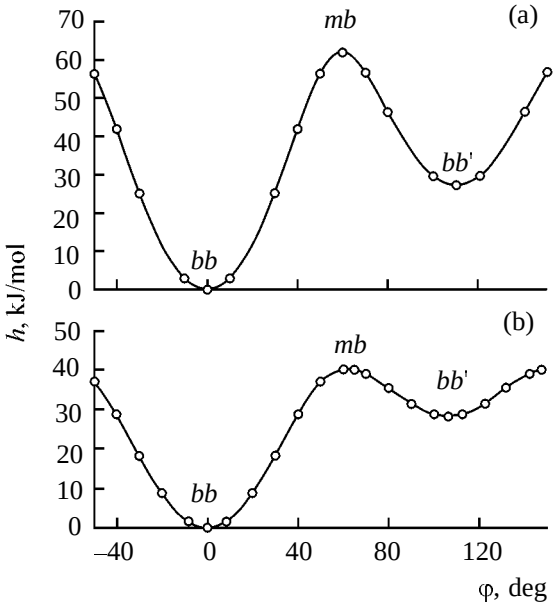

Fig. 2. Minimum-energy pathways of the intramolecular rearrangement *bb*(D_{2d}) → *mb*(C_1) → *bb*'(C_s) in (a) Li_2SO_4 and (b) K_2WO_4 molecules. The reaction coordinate φ is the dihedral angle describing deviation of the M atom from the XO_2 plane.

Table 3. Vibration frequencies (ω_i, cm^{-1}) and IR intensities (A_i, km mol^{-1}, in parentheses) for M_2XO_4 molecules (X = S, Se, Te)

Parameter	Li_2SO_4	Na_2SO_4	K_2SO_4	Li_2SeO_4	Na_2SeO_4	K_2SeO_4	Li_2TeO_4	Na_2TeO_4	K_2TeO_4
				bb(D_{2d}) structure					
ω_1 (A_1)	1060	1054	1057	914	908	910	818	813	815
ω_2 (A_1)	668	575	544	611	488	452	573	422	382
ω_3 (A_1)	499	281	201	444	263	189	400	250	179
ω_4 (B_2)	1276 (526)	1250 (604)	1241 (700)	995 (223)	978 (279)	975 (319)	874 (161)	864 (202)	863 (228)
ω_5 (B_2)	758 (81)	729 (76)	706 (106)	590 (471)	552 (151)	524 (182)	557 (448)	452 (193)	420 (219)
ω_6 (B_2)	612 (418)	360 (140)	279 (133)	568 (44)	323 (101)	246 (94)	477 (64)	297 (74)	223 (70)
ω_7 (B_1)	418	439	450	309	330	340	228	244	253
ω_8 (E)	1207 (915)	1205 (966)	1207 (875)	946 (440)	951 (460)	953 (417)	834 (316)	839 (324)	842 (301)
ω_9 (E)	668 (163)	666 (123)	669 (115)	511 (269)	482 (200)	479 (185)	440 (312)	378 (271)	368 (251)
ω_{10} (E)	410 (21)	270 (10)	213 (10)	361 (5)	250 (1)	197 (3)	319 (83)	227 (3)	177 (0)
ω_{11} (E)	159 (191)	69 (123)	42 (93)	154 (139)	67 (97)	41 (75)	151 (61)	73 (68)	45 (57)
				bb'(C_s) structure					
ω_1 (A')	1405 (414)	1344 (442)	1298	1060 (153)	1032 (174)	1016 (183)	898 (85)	890 (104)	886 (117)
ω_2 (A')	1105 (254)	1114 (316)	1130	915 (60)	917 (76)	922 (77)	815 (30)	816 (41)	819 (45)
ω_3 (A')	989 (299)	1001 (253)	1024	842 (252)	848 (229)	864 (188)	764 (228)	770 (198)	781 (165)
ω_4 (A')	717 (102)	692 (53)	679	612 (259)	520 (120)	497 (117)	578 (241)	434 (161)	402 (159)
ω_5 (A')	658 (73)	660 (70)	665	538 (8)	477 (104)	477 (93)	476 (59)	376 (137)	368 (124)
ω_6 (A')	619 (122)	482 (2)	483	491 (146)	374 (0)	373 (0)	418 (185)	303 (4)	282 (2)
ω_7 (A')	438 (12)	320 (50)	235	337 (11)	288 (34)	216 (29)	292 (15)	252 (26)	202 (25)
ω_8 (A')	369 (24)	187 (17)	108	320 (0)	179 (8)	112 (9)	246 (8)	168 (1)	112 (4)
ω_9 (A')	193 (91)	80 (46)	32	189 (61)	83 (35)	47 (23)	184 (21)	93 (22)	57 (16)
ω_{10} (A'')	1239 (494)	1242 (543)	1252	966 (222)	966 (253)	970 (266)	848 (162)	850 (183)	853 (192)
ω_{11} (A'')	722 (126)	705 (73)	691	614 (260)	546 (123)	514 (152)	576 (218)	464 (130)	419 (159)
ω_{12} (A'')	640 (96)	533 (3)	503	547 (5)	421 (2)	401 (0)	486 (46)	343 (12)	319 (14)
ω_{13} (A'')	480 (81)	323 (42)	261	423 (55)	295 (11)	238 (12)	397 (31)	258 (18)	210 (14)
ω_{14} (A'')	444 (24)	303 (50)	235	377 (20)	275 (56)	212 (53)	295 (44)	253 (44)	187 (36)
ω_{15} (A'')	157 (10)	56 (0)	51*i*	162 (8)	68 (0)	19 (0)	178 (3)	89 (1)	57 (0)

the use of the Hartree–Fock equilibrium geometries in the CISD+Q calculations will also be insignificant.

Comparison of the relative energies *h*(*bb*') and *h*(*tt*) calculated by the HF and CISD+Q methods (Tables 1, 2) shows that in most cases taking into account the electron correlation decreases the relative energy of the "excited" configurations (by 2–20 kJ mol^{-1}). The exceptions are the *tt* configurations of the Na_2MoO_4 and Na_2WO_4 molecules, for which *h*(*tt*) remains unchanged or slightly increases when the electron correlation is taken into account. It should be noted that for molecules with low relative energies of "excited" configurations the CI calculations give appreciably decreased values of *h*. For example, in going from HF to CISD+Q calculations, for K_2SO_4 $h(tt) = E(tt) - E(bb)$ decreases from 21 to 13 kJ mol^{-1}.

Force fields and vibration spectra of M_2XO_4 molecules. The calculated vibration frequencies and intensities in the IR spectra of M_2XO_4 molecules are listed in Tables 3 and 4. The vibrational representations of the M_2XO_4 molecule with the structures of the D_{2d} and C_s symmetry are $3A_1 + B_1 + 3B_2 + 4E$ and $9A' + 6A''$, respectively. We used the system of vibrational coordinates of the M_2XO_4 molecules described in [14].

Analysis of the normal modes and distribution of the vibrational potential energy throughout the vibrational coordinates shows that many vibrations of the M_2XO_4 molecules are appreciably mixed (to a greater extent in Li_2XO_4 and to a lesser extent in K_2XO_4) and therefore cannot be interpreted unambiguously. Nevertheless, we can conventionally distinguish nine normal modes of the M_2XO_4 molecule correlating with vibrations of the XO_4^{2-} tetrahedron (vibrational representation $A_1 + E + 2F_2$). The remaining six modes correspond to motion of the M^+ cations relative to the XO_4^{2-} anion. The correlations between the vibrations of the free XO_4^{2-} ion and those of the XO_4^{2-} ion in the

Table 4. Vibration frequencies (ω_i, cm^{-1}) and IR intensities (A_i, km mol^{-1}, in parentheses) for M_2XO_4 molecules (X = Cr, Mo, W)

Parameter	Li_2CrO_4	Na_2CrO_4	K_2CrO_4	Li_2MoO_4	Na_2MoO_4	K_2MoO_4	Li_2WO_4	Na_2WO_4	K_2WO_4
				bb(D_{2d}) structure					
ω_1 (A_1)	1036	1024	1027	1002	994	995	1027	1019	1022
ω_2 (A_1)	622	485	459	580	432	405	579	435	410
ω_3 (A_1)	460	270	200	428	262	192	436	264	193
ω_4 (B_2)	1041 (639)	1014 (733)	1011 (815)	942 (723)	923 (778)	919 (827)	924 (614)	908 (647)	906 (682)
ω_5 (B_2)	603 (421)	523 (18)	507 (18)	574 (411)	449 (62)	427 (66)	573 (397)	436 (95)	413 (103)
ω_6 (B_2)	571 (95)	335 (153)	264 (143)	492 (96)	310 (124)	239 (110)	472 (83)	295 (92)	224 (82)
ω_7 (B_1)	364	375	379	309	318	322	308	319	324
ω_8 (E)	948 (933)	986 (1059)	987 (980)	888 (894)	899 (996)	898 (933)	861 (514)	887 (836)	889 (787)
ω_9 (E)	456 (27)	438 (4)	437 (3)	390 (124)	361 (52)	359 (45)	386 (138)	346 (87)	343 (77)
ω_{10} (E)	386 (2)	254 (2)	207 (3)	344 (1)	224 (0)	181 (1)	313 (2)	218 (0)	177 (1)
ω_{11} (E)	170 (157)	67 (107)	47 (82)	168 (86)	75 (85)	51 (67)	158 (44)	72 (77)	49 (59)
				bb'(C_s) structure					
ω_1 (A')	1194 (400)	1145 (406)	1122 (403)	1079 (268)	1053 (245)	1038 (214)	1076 (132)	1056 (110)	1047 (87)
ω_2 (A')	1026 (165)	1017 (189)	1018 (184)	958 (288)	950 (326)	947 (352)	953 (340)	944 (368)	941 (392)
ω_3 (A')	837 (426)	832 (494)	855 (470)	790 (446)	789 (496)	806 (471)	800 (387)	796 (417)	813 (396)
ω_4 (A')	612 (174)	469 (16)	460 (10)	582 (168)	409 (60)	393 (45)	580 (172)	405 (78)	386 (62)
ω_5 (A')	504 (24)	432 (4)	434 (3)	452 (59)	361 (33)	356 (30)	445 (57)	350 (43)	343 (39)
ω_6 (A')	434 (17)	397 (10)	395 (4)	378 (63)	330 (6)	331 (1)	372 (87)	320 (11)	326 (14)
ω_7 (A')	367 (1)	303 (39)	232 (40)	312 (1)	285 (28)	218 (32)	311 (3)	278 (24)	209 (24)
ω_8 (A')	351 (2)	188 (10)	127 (10)	288 (3)	166 (6)	115 (7)	262 (2)	153 (5)	109 (5)
ω_9 (A')	199 (66)	85 (37)	57 (22)	187 (33)	91 (26)	60 (17)	174 (28)	88 (24)	57 (15)
ω_{10} (A'')	1044 (572)	1027 (639)	1021 (669)	928 (577)	917 (637)	912 (652)	904 (495)	897 (541)	895 (553)
ω_{11} (A'')	615 (245)	514 (27)	486 (22)	569 (234)	448 (59)	415 (60)	567 (204)	445 (64)	411 (68)
ω_{12} (A'')	534 (15)	435 (16)	425 (16)	486 (11)	363 (1)	356 (0)	479 (24)	350 (2)	346 (6)
ω_{13} (A'')	423 (0)	300 (46)	239 (16)	371 (2)	278 (50)	219 (39)	362 (25)	277 (39)	218 (25)
ω_{14} (A'')	411 (5)	289 (22)	235 (60)	347 (7)	251 (4)	197 (20)	331 (3)	236 (12)	181 (24)
ω_{15} (A'')	182 (14)	72 (1)	47 (0)	198 (10)	92 (2)	66 (0)	193 (7)	92 (1)	66 (0)

ground isomer *bb*(D_{2d}) of the M_2XO_4 molecules are shown below:

$$\omega_1\ (A_1) \longrightarrow \omega_1\ (A_1),$$

$$\omega_2\ (E) \longrightarrow \omega_3\ (A_1) + \omega_7\ (B_1) \text{ for M = Li,}$$

or

$$\omega_2\ (A_1) + \omega_7\ (B_1) \text{ for M = Na, K,}$$

$$\omega_3\ (F_2) \longrightarrow \omega_4\ (B_2) + \omega_8\ (E),$$

$$\omega_4\ (F_2) \longrightarrow \omega_6\ (B_2) + \omega_9\ (E) \text{ for M = Li,}$$

or

$$\omega_5\ (B_2) + \omega_9\ (E) \text{ for M = Na, K.}$$

The strongest bands in the IR spectra of M_2XO_4 molecules are those originating from vibrations of the XO_4 fragment, and the weakest bands originate from the motion of M^+ cations relative to the XO_4^{2-} anion.

In the series $Li_2XO_4 \rightarrow Na_2XO_4 \rightarrow K_2XO_4$, the force constants of M–O stretching and XO_2M out-of-plane bending (along the coordinate χ [12]) considerably decrease. For example, the constant f_χ for the M_2SO_4 molecules of the *bb*(D_{2d}) structure decreases from 0.078 mdyne Å for M = Li to 0.027 mdyne Å for M = K. At the same time, the force constansts describing the dynamics of the XO_4 fragment vary less significantly. Similar trends were also observed with the corresponding vibration frequencies (Tables 3, 4).

The possible CI corrections to the Hartree–Fock frequencies and IR intensities for the M_2XO_4 molecules can be evaluated by comparing the results of calculating these quantities by the HF (Table 3) and CISD+Q methods. The vibrational frequencies ω_i (cm^{-1}) found in the CISD+Q approximation and the IR intensities A_i (km mol^{-1}, found in the CISD approximation, given in parentheses) for the ground isomer *bb*(D_{2d}) of the Li_2SO_4 molecule are as follows (i = 1–11): 968, 649, 466, 1184 (469), 697 (93), 600

Table 5. Vibration frequencies (ν_i, cm^{-1}) of matrix-isolated M_2XO_4 molecules

Molecule	ν_1 (A_1)	ν_4 (B_2)	ν_5 (B_2)	ν_6 (B_2)	ν_8 (E)	ν_9 (E)	ν_{10} (E)
Li_2SO_4	–	1140[a]	–	–	1101[a]	–	–
Na_2SO_4	961[b]	1134–1137[c]	640[b]	–	1100[c]	610[b]	295[c]
K_2SO_4[d]	962[b]	1128[c]	640[c]	262[c]	1099[c]	608[c]	220–240[c]
Rb_2SO_4	–	1122–1128[c]	636[c]	215[c]	1096–1100[c]	608[c]	190–200[c]
Cs_2SO_4	962[e]	1125[c]	631–635[c]	196[c]	1090–1100[c]	610[c]	148–170[c]
M_2SeO_4[f]	–	880–881	377–389	–	894	438–445	–
M_2CrO_4[g]	–	895–898	–	–	877	–	–
K_2CrO_4	853[e]	893[h]	429[h]	248[h]	875[h]	–	–
Rb_2CrO_4	–	890[i]	–	–	877[i]	–	–
Cs_2CrO_4	847[e]	889[i]	–	–	876[i]	–	–
M_2MoO_4[g]	–	840–844	–	–	830	–	–
K_2MoO_4	886[e]	839[h]	378[h]	227[h]	827[h]	318[h]	–
Rb_2MoO_4	–	839[i]	–	–	830[i]	–	–
Cs_2MoO_4	891[e]	839[a]	–	–	830[a]	–	–
Li_2WO_4	–	839[a]	–	–	830[a]	–	–
Na_2WO_4	–	836[a]	376[j]	–	830[a]	306[j]	–
K_2WO_4	925[e]	836[a]	351[a]	218[h]	831[a]	306[a]	–
Rb_2WO_4	–	836[i]	–	–	830[i]	–	–
Cs_2WO_4	925[e]	835[a]	–	–	830[a]	–	–

[a] IR spectrum (N_2 matrix) [6]. [b] Raman spectrum (N_2) [6]. [c] IR spectrum (Ar) [5]. [d] IR spectrum [5]: ν_1 (E) 70–82 (Xe), 65–85 (Kr), and 57–67 (Ar) cm^{-1}. [e] Raman spectrum (Ne) [9]. [f] M = Na, K, Rb, Cs; IR spectrum (N_2) [10]. [g] M = Li, Na; IR spectrum (N_2) [6]. [h] IR spectrum (Ar) [7]. [i] IR spectrum (N_2) [8]. [j] IR spectrum (Ar) [6].

(400), 373, 1100 (820), 613 (144), 409 (10), and 147 (185). Thus, taking into account electron correlation decreases by 0.2–11% the frequencies ω_i and only weakly affects the IR intensities.

Comparison of the results of *ab initio* calculations with the experiment. The results of mass-spectrometric study of the vapors of alkali metal sulfates [22], selenates [10], chromates [22, 23], molybdates [22], and tungstates [22, 24] in a wide temperature range (800–2000 K) show that these compounds vaporize without significant decomposition and exist in the gas phase mainly as monomeric molecules M_2XO_4.

Let us now compare the results of *ab initio* calculations of the vibration spectra of M_2XO_4 molecules with the experimental IR and Raman spectra of species obtained by vaporization of M_2XO_4 salts and isolated in inert matrices [5–10]. The experimental frequencies [5–10], listed in Table 5, are consistent with the bisbidentate (D_{2d}) structure of the M_2XO_4 molecules. Alkali metal sulfates have been studied most extensively; e.g., for K_2SO_4 the frequencies of all the IR-active normal modes and of the Raman-active ν_1 (A_1) mode are known from the experiment. Data on vibration spectra of the M_2TeO_4 and Li_2SeO_4 molecules are lacking. For the majority of the other M_2XO_4 molecules, only the frequencies of the XO_4 fragments are known; the results of *ab initio* calculations agree with these data. The IR spectra of K_2XO_4 molecules (X = Cr, Mo, W) isolated in an argon matrix contained in the low-frequency range corresponding to metal–oxygen stretching vibrations a single band [7] assignable, according to our calculations, to the ω_6 (B_2) K–O vibrations of the D_{2d} isomer of the K_2XO_4 molecules.

The vibration frequencies of the M_2XO_4 molecules calculated by us systematically exceed the experimental frequencies: by 3–10% for stretching modes and by 12–15% for bending modes. Such a deviation from the experiment is due, on the one hand, to insufficient completeness of the set of basis functions used in our calculations, possible defects of the effective core potentials, and neglect of the electron correlation and of the anharmonicity effects and, on the other hand, to certain difference between the vibration frequencies of matrix-isolated and free molecules.

In view of the results of our study, interpretation of the vibration spectra of M_2XO_4 molecules made in spectroscopic studies [5–10] assuming existence of a single structure of these molecules seems to be incomplete. In the IR spectra of M_2XO_4 molecules a number of additional bands were observed [5, 7], both in the range of X–O stretching vibrations and in the low-

Table 6. Apparent internuclear distances and bond angles in the M_2XO_4 molecules, determined by high-temperature gas-phase electron diffraction

Molecule	R_g(MO), Å	R_g(XO), Å	α_g(OXO), deg	Vapor temperature, K	References
K_2SO_4	2.45 ± 0.03	1.47 ± 0.01	109 ± 10	1670 ± 100	[1]
Cs_2SO_4	2.60 ± 0.03	1.48 ± 0.01	109 ± 10	1670 ± 100	[1]
Cs_2SO_4	2.80 ± 0.05	1.471 ± 0.004	109 ± 4	1320	[3]
K_2CrO_4	2.45 ± 0.03	1.66 ± 0.01	109 ± 10	1370 ± 100	[1]
Cs_2CrO_4	2.85 ± 0.04	1.675 ± 0.006	108 ± 2	1470 ± 50	[4]
Rb_2MoO_4	2.74 ± 0.02	1.779 ± 0.009	101 ± 2	1170 ± 30	[2]
Cs_2MoO_4	2.80 ± 0.03	1.80 ± 0.02	105 ± 4	1320 ± 30	[2]
Rb_2WO_4	2.69 ± 0.02	1.798 ± 0.009	104 ± 2	1070 ± 30	[2]
Cs_2WO_4	2.78 ± 0.04	1.82 ± 0.02	104 ± 4	1170 ± 30	[2]

frequency range. These bands were not unambiguously assigned in [5, 7]. Our results suggest that some of these bands can be assigned to vibrations of the XO_4 fragments in the C_s isomers of the M_2XO_4 molecules.

The molecules of potassium, rubidium, and cesium sulfates, chromates, molybdates, and tungstates were studied by high-temperature gas-phase electron diffraction in [1–4] (Table 6). Before comparing the results of our calculations with those of electron diffraction studies, three facts should be noted.

(1) The error in calculating the equilibrium internuclear distances, originating form insufficiently high level of the theory used (incompleteness of basis sets, neglect of electron correlation, possible defecrts of the effective core potentials) can be significant (up to 0.02–0.03 Å). At the same time, the error in determining the relative geometries can be much lower, because calculations for all the molecules are performed on the same level of theory using similar effective core potentials and basis sets. Therefore, we believe that the trends in variation of the molecular parameters in the series $Li_2XO_4 \rightarrow Na_2XO_4 \rightarrow K_2XO_4$, $M_2SO_4 \rightarrow M_2SeO_4 \rightarrow M_2TeO_4$, and $M_2CrO_4 \rightarrow M_2MoO_4 \rightarrow M_2WO_4$, and also in going from $M_2X^{(p)}O_4$ ($X^{(p)}$ = S, Se, Te) to $M_2X^{(d)}O4$ ($X^{(d)}$ = Cr, Mo, W) molecules are predicted with a fairly high accuracy, on a quantitative level.

(2) The internuclear distances R_g(A–B) determined by electron diffraction are apparent quantities. Namely, R_g(A–B) is the distance between nuclei A and B, averaged over all the vibrational states of the thermally equilibrium (i.e., described by the Boltzmann distribution) molecular ensemble. The apparent distance R_g(A–B) differs from the equilibrium internuclear distance R_e(A–B). The correction $\Delta R = R_g - R_e$ depends on temperature and on the structure and force field of the molecule. This correction can be different for different pairs of nuclei. For "chemically bound" pairs of atoms, these corrections are usually positive. In the M_2XO_4 molecules at temperatures of electron diffraction experiments (1100–1800 K) the corrections $\Delta R = R_g - R_e$ to the internuclear distances X–O and M–O can be significant (~0.02–0.03 Å, according to our estimates). In view of the facts that all the molecules M_2XO_4 studied by gas-phase electron diffraction have similar structures and similar force fields and that the temperatures at which the electron diffraction patterns were taken (Table 6) differ not very strongly, the correction $\Delta R = R_g - R_e$ can be expected to be similar for the pairs of nuclei of the same type in different M_2XO_4 molecules. Hence, for structurally similar M_2XO_4 molecules, comparison of trends in variation of the theoretical equilibrium internuclear distances R_e with the experimental data on apparent distances R_g is quite justified and can furnish useful information on the reliability of both experimental R_g values and theoretical predictions.

(3) In all the electron diffraction studies of M_2XO_4 molecules [1–4], the diffraction patterns were interpreted assuming a structure with four symmetrically equivalent X–O distances and four symmetrically equivalent M–O distances (D_{2d} structure). Thus, in none of the electron diffraction studies [1–4] the possible coexistence of the D_{2d} isomer with the C_s isomer, predicted by the theory for all the M_2XO_4 molecules except K_2SO_4 (and probably also Rb_2SO_4 and Cs_2SO_4), was taken into account. At the same time, according to our estimates [14], under conditions of thermodynamic equilibrium the concentration of the $bb'(C_s)$ isomer of the M_2WO_4 molecules in the gas phase of rubidium and cesium tungstates can be comparable with that of the ground $bb(D_{2d})$ isomer: at temperatures of electron diffraction measurements [2], the relative content of the $bb'(C_s)$ isomer should be about 30% for Rb_2WO_4 (1070 K) and 34% for

Cs_2WO_4 (1170 K). Significant concentrations of the excited isomers should also be expected for the other M_2XO_4 molecules. For example, in potassium chromate vapor at the temperature of electron diffraction measurements [1] (1370 K) the content of the $bb'(C_s)$ isomer, estimated from the thermodynamic functions that were calculated from the molecular constants found in this work, is as high as ~57%. Let us consider how the presence of the $bb'(C_s)$ isomer of gaseous M_2XO_4 molecules can disturb the geometries of these compounds evaluated assuming the $bb(D_{2d})$ isomer as the sole species. Comparison of the equilibrium geometries of the *bb* and *bb'* isomers (Tables 1, 2) shows that the $R_e(X–O)_{bb}$ distance in the *bb* isomer and the average $R_e(X–O)$ distance in the *bb'* isomer $[R_e^{av}(X–O)_{bb'}]$ are approximately equal: $R_e^{av}(X–O)_{bb'}$ exceeds $R_e(X–O)_{bb}$ by only 0.001–0.007 Å, with this difference tending to decrease in the series $Li_2XO_4 \rightarrow Na_2XO_4 \rightarrow K_2XO_4$. The average O···O distances are also similar: $R_e^{av}(O\cdots O)_{bb'}$ differs from $R_e^{av}(O\cdots O)_{bb}$ in the M_2XO_4 molecules, on the average, by 0.003 Å, with the largest differnce (in the Li_2TeO_4 molecule) being 0.015 Å. Hence, the structural parameters $R_g(X–O)$ and $R_g(O\cdots O)$ of the XO_4 fragment of the M_2XO_4 molecule, obtained when the electron scattering patterns of a mixture of the *bb* and *bb'* isomers are interpreted assuming existence of the *bb* isomer as a sole species, should not differ significantly from the actual structural parameters of the XO_4 fragment in the *bb* isomer. As for the alkali metal–oxygen distances, in Li_2XO_4 molecules the average distance $R_e^{av}(M–O)_{bb'}$ in the *bb'* isomer is somewhat shorter than the $R_e(M–O)_{bb}$ distance in the *bb* isomer, whereas in Na_2XO_4 and K_2XO_4 molecules it is slightly longer [for example, in the K_2CrO_4 molecule the difference $R_e^{av}(M–O)_{bb'} - R_e(M–O)_{bb}$ is 0.014 Å]. The trends in variation of the metal–oxygen distances in the *bb* and *bb'* isomers in the series $Li_2XO_4 \rightarrow Na_2XO_4 \rightarrow K_2XO_4$ suggest that in Rb_2XO_4 and Cs_2XO_4 molecules the $R_e^{av}(M–O)_{bb'}$ distances should be longer than the $R_e(M–O)_{bb}$ distances by 0.02–0.03 Å. This fact suggests that for M = K, Rb, and Cs the parameter $R_g(M–O)$ of the M_2XO_4 molecules obtained from the electron diffraction data without taking isomerism into consideration will be somewhat overestimated. At the expected concentrations of the *bb'* isomer the overestimation can reach 0.01–0.02 Å.

Note that the errors in estimating the apparent (obtained without considering isomerism) root-mean-square vibration amplitudes of the nuclei in M_2XO_4 molecules should be considerably more significant. These errors originate from line broadening in the radial distribution curves $f(R)$ for the total diffraction pattern as compared to the curve $f(R)_{bb}$ corresponding to electron scattering on the *bb* molecules only. The broadening is due to summation of two functions: $f(R)_{bb}$ from the *bb* isomer and $f(R)_{bb'}$ from the *bb'* isomer. Furthermore, the structural peaks in the $f(R)_{bb'}$ curve should consist of several components. For example, in the radial distribution curve $f(R)_{bb'}$ the peak corresponding to the M–O distance will consist of two peaks (M–O and M–O'), and the peak corresponding to the X–O distance, of three peaks (X–O, X–O', and X–O'') (Fig. 1; Tables 1, 2). In what follows we discuss only the internuclear distances obtained in electron diffraction experiments (the experimental and theoretical mean vibration amplitudes in alkali metal tungstates are compared in our previous paper [14]).

On the whole, the above arguments show that comparison of the internuclear distances in M_2XO_4 molecules, determined experimentally by electron diffraction [1–4] and calculated *ab initio* for the ground isomer $bb(D_{2d})$, is justified. However, additional discussion is required for the Rb_2SO_4 and Cs_2SO_4 molecules, because the results of our calculations do not rule out the existence of the bistridentate (*tt*, C_{2v} symmetry) isomer of these molecules, close to the $bb(D_{2d})$ isomer in energy. Comparison of the internuclear distances in the $bb(D_{2d})$ and $tt(C_{2v})$ structures (Tables 1, 2) shows that the average X–O and O···O distances in both structures differ insignificantly. At the same time, the metal–oxygen distances in the $tt(C_{2v})$ isomer are considerably longer than those in the $bb(D_{2d})$ isomer: the difference $R_e^{av}(K–O)_{tt} - R_e(K–O)_{bb}$ in the K_2SO_4 molecule is as large as 0.175 Å. For Rb_2SO_4 and Cs_2SO_4, the difference between the metal–oxygen distances in the $tt(C_{2v})$ and $bb(D_{2d})$ structures should be similar or even greater. Hence, if the content of the $tt(C_{2v})$ isomer in the vapors of rubidium and cesium sulfates is significant, the apparent metal–oxygen distance determined by gas-phase electron diffraction without taking into account the isomerism of the Rb_2SO_4 and Cs_2SO_4 molecules should appreciably exceed the distance expected for the $bb(D_{2d})$ isomer.

Let us start comparison of the calculation results and electron diffraction data with structural parameters of the XO_4 fragment. Our calculations show that in the series $Li_2XO_4 \rightarrow Na_2XO_4 \rightarrow K_2XO_4$ the $R_e(X–O)$ distance is approximately constant, which allows us to expect that in going to the rubidium (Rb_2XO_4) and cesium (Cs_2XO_4) salts it will not appreciably change either. This conclusion is consistent with the electron diffraction data (Table 6): The $R_g(X–O)$ distances (within determination error) are the same in molecules with different M. Variation of the theoretical X–O distances $R_e(X–O)$ in the series $M_2CrO_4 \rightarrow M_2MoO_4 \rightarrow M_2WO_4$ agrees with experimentally observed variation

of R_g(X–O): R_e(Mo–O) – R_e(Cr–O) = 0.15 Å for K_2XO_4 (Table 2), R_g(Mo–O) – R_g(Cr–O) = 0.12 ± 0.03 Å for Cs_2XO_4 (Table 6); R_e(W–O) – R_e(Mo–O) = 0.01 Å for K_2XO_4 (Table 2), R_g(W–O) – R_g(Mo–O) = 0.02 ± 0.02 Å for Rb_2XO_4 and Cs_2XO_4 (Table 6). The experimental parameters R_g(X–O) of the M_2CrO_4, M_2MoO_4, and M_2WO_4 molecules exceed the theoretical R_e(X–O) values by 0.06 – 0.07 (X = Cr) or 0.03–0.05 Å (X = Mo, W). This discrepancy is not very large, taking into account the expected corrections ΔR(X–O) = R_g(X–O) – R_e(X–O) and the errors of R_g^{exp} and R_e^{theor}. At the same time, for alkali metal sulfate molecules comparison of the theoretical (R_e) and experimental (R_g) S–O distances, taking into account the similar corrections and possible errors, shows that the theoretical data are not quite consistent with the experiment: the experimental R_g(S–O) values are lower by 0.03–0.04 Å than those predicted by the theory. The theoretical bond angles α_e(OXO) in the M_2XO_4 molecules of the D_{2d} symmetry agree with the experimental α_g(OXO) values.

Let us now compare the metal–oxygen distances. Direct comparison can be performed for two molecules only: K_2SO_4 and K_2CrO_4. The R_g(K–O) distances in the potassium sulfate and chromate molecules, according to [1], are equal within the determination error (± 0.03 Å). Our calculations give a similar result: In the K_2SO_4 and $KrCrO_4$ molecules of the D_{2d} symmetry, R_e(K–O) differs by only 0.015 Å (Tables 1, 2). At the same time, the absolute values of the K–O distances calculated by us and found in [1] differ considerably: The measured R_g(K–O) values are 0.07–0.09 Å lower than the theoretical R_e(K–O) values. After taking into account the correction ΔR = R_g – R_e, this discrepancy becomes even larger, reaching 0.10–0.12 Å, which considerably exceeds the total error in R_g and R_e. Thus, our calculations suggest that the parameters R_g(K–O) obtained in [1] for K_2SO_4 and K_2CrO_4 are erroneous.

The metal–oxygen distances in the molecules of rubidium and cesium salts M_2XO_4 determined by gas-phase electron diffraction can be compared to the calculated M–O distances in the corresponding molecules with lighter alkali metal using the above-mentioned system of ionic radii from [21]. The R_e(M–O) distance in the Rb_2XO_4 and Cs_2XO_4 can be estimated by the formula:

$$R_e(M–O) = R_e(K–O) + R(M^+) – R(K^+), \qquad (2)$$

where M = Rb or Cs, R_e(K–O) is the K–O distance in the corresponding K_2XO_4 molecule calculated by us, and $R(M^+)$ and $R(K^+)$ are the ionic radii from [21].

The R_e(Rb–O) distances in the ground (D_{2d}) isomers of the Rb_2MoO_4 and Rb_2WO_4 molecules, calculated by this procedure, are 2.70 and 2.71 Å, respectively. The former value agrees with the distance R_g(Rb–O) = 2.74 ± 0.02 Å in the Rb_2MoO_4 molecule, measured in [2]. However, the value of 2.69 ± 0.02 Å obtained in the same study [2] for R_e(Rb–O) in Rb_2WO_4 is probably erroneous: it is appreciably lower than R_g(Rb–O) expected by us (~2.75 Å) and contradicts the trend, revealed by *ab initio* calculations, toward an increase in the alkali metal–oxygen distance in going from molybdates to tungstates.

Calculation by formula (2) gives the following M–O internuclear distance in the D_{2d} isomers of Cs_2XO_4 molecules: R_e(Cs–O) 2.76 Å in Cs_2SO_4, 2.77 Å in Cs_2CrO_4, 2.82 Å in Cs_2MoO_4, and 2.83 Å in Cs_2WO_4. The value of R_e(Cs–O) estimated for Cs_2SO_4 is quite consistent with R_g(Cs–O) = 2.80 ± 0.05 Å, measured for this molecule by electron diffraction [3], and both the result of [3] and calculated value contradict the R_g(Cs–O) distance found for Cs_2SO_4 in [1]: 2.60 ± 0.03 Å. This fact supports our conclusion that the metal–oxygen distances in M_2XO_4 molecules determined by electron diffraction in [1] are erroneous. Furthermore, agreement between the theoretically predicted Cs–O distance in the D_{2d} isomer of the Cs_2SO_4 molecule and the experimental value [3] shows that the D_{2d} isomer is, indeed, the ground isomer of Cs_2SO_4 and that no significant amounts of the $tt(C_{2v})$ isomer are present. The same conclusion is apparently valid for Rb_2SO_4.

The R_e(Cs–O) distance evaluated by us for the $bb(D_{2d})$ isomer of the Cs_2CrO_4 molecule is 0.08 Å shorter than the apparent experimental [4] R_g(Cs–O) distance, 2.85 ± 0.04 Å. The difference $R_g^{exp} – R_e^{theor}$ = 0.08 Å exceeds the expected correction for this pair of nuclei ΔR = R_g – R_e. Such a difference between the observed apparent (obtained without considering isomerism) Cs–O distance in the Cs_2CrO_4 molecule and the R_e(Cs–O) distance theoretically predicted for the $bb(D_{2d})$ isomer of this molecule is an indirect evidence of an appreciable content of the $bb'(C_s)$ isomer of Cs_2CrO_4 in the phase of cesium chromate. However, the deviation of the theoretical prediction from the experiment can also be due to significant errors in determination of R_g^{exp} and calculation of R_e^{theor}.

In the light of our results, the R_g(Cs–O) in the Cs_2MoO_4 and Cs_2WO_4 molecules measured in [2] (Table 6) seem to be appreciably underestimated (by 0.05–0.10 Å); the same is true for the R_g(Rb–O) distance in the Rb_2WO_4 molecule, measured in [2].

To conclude: Unfortunately, available structural data obtained for M_2XO_4 molecules by gas-phase electron diffraction are often insufficiently reliable.

This is primarily due to problems with interpretation of high-temperature electron diffraction patterns of nonrigid molecules. Large vibration amplitudes smear the diffraction patterns, and the structural information related to distances between the alkali metal atoms and atoms of the XO_4 fragment is "washed out." Another complicating factor is the structural isomerism of the M_2XO_4 molecules, which was taken into account in none of the published electron diffraction studies.

We believe that it would be useful to perform additional diffraction and spectroscopic studies of M_2XO_4 molecules and interpret the results taking into account the structural features of these molecules revealed in this work.

ACKNOWLEDGMENTS

The work was supported by the Ministry of Education of the Russian Federation (Competitive Center for Basic Research, St. Petersburg State University), project no. 97-0-9.1-262.

REFERENCES

1. Spiridonov, V.P. and Lutoshkin, B.N., *Vestn. Mosk. Gos. Univ., Ser. 2: Khim.,* 1970, vol. 11, no. 5, pp. 509–512.
2. Ezhov, Yu.S. and Sarvin, A.P., *Zh. Strukt. Khim.,* 1980, vol. 21, no. 5, pp. 40–45.
3. Kulikov, V.A., Ugarov, V.V., and Rambidi, N.G., *Zh. Strukt. Khim.,* 1982, vol. 23, no. 1, pp. 184–187.
4. Girichev, G.V., Giricheva, N.I., Kuligin, E.A., and Krasnov, K.S., *Zh. Strukt. Khim.,* 1983, vol. 24, no. 1, pp. 63–69.
5. Dvorkin, M.I., *Cand. Sci. (Phys.–Math.) Dissertation,* Leningrad, 1977.
6. Spoliti, M., in *Matrix Isolation Spectroscopy. Lectures and Discussions (Montpellier, 1980),* Dordrecht: NATO Adv. Study Inst., 1981, pp. 473–484.
7. Beattie, I.R., Ogden, J.S., and Price, D.D., *J. Chem. Soc., Dalton Trans.,* 1982, no. 3, pp. 505–510.
8. Bencivenni, L. and Gingerich, K.A., *J. Chem. Phys.,* 1982, vol. 76, no. 1, pp. 53–56.
9. Nagarathna, H.M., Bencivenni, L., and Gingerich, K.A., *J. Chem. Phys.,* 1984, vol. 81, no. 2, pp. 591–598.
10. Brisdon, A.K., Gomme, R.A., and Ogden, J.S., *J. Phys. Chem.,* 1991, vol. 95, no. 7, pp. 2927–2931.
11. Ramondo, F., Bencivenni, L., Caminiti, R., and Sadun, C., *Chem. Phys.,* 1991, vol. 151, no. 2, pp. 179–186.
12. Sliznev, V.V. and Solomonik, V.G., *Koord. Khim.,* 1996, vol. 22, no. 9, pp. 699–705.
13. Marenich, A.V. and Solomonik, V.G., *Zh. Neorg. Khim.,* 2001, vol. 46, no. 3, pp. 462–466.
14. Solomonik, V.G. and Marenich, A.V., *Zh. Fiz. Khim.,* 2000, vol. 74, no. 1, pp. 94–102.
15. Schmidt, M.W., Baldridge, K.K., Boatz, J.A., Elbert, S.T., Gordon, M.S., Jensen, J.H., Koseki, S., Matsunaga, N., Nguyen, K.A., Su, S.J., Windus, T.L., Dupuis, M., and Montgomery, J.A., *J. Comput. Chem.,* 1993, vol. 14, no. 11, pp. 1347–1363.
16. Stevens, W.J., Basch, H., and Krauss, M., *J. Chem. Phys.,* 1984, vol. 81, no. 12, pp. 6026–6033.
17. Stevens, W.J., Krauss, M., Basch, H., and Jasien, P.G., *Can. J. Chem.,* 1992, vol. 70, no. 2, pp. 612–630.
18. Huzinaga, S., Andzelm, J., Klobukowski, M., Radzio-Andzelm, E., Sakai, J., and Tatewaki, H., *Gaussian Basis Sets for Molecular Calculations (Phys. Sci. Data, vol. 16),* Amsterdam: Elsevier, 1984, vol. 8.
19. Davidson, E.R. and Silver, D.W., *Chem. Phys. Lett.,* 1977, vol. 52, no. 3, pp. 403–406.
20. Solomonik, V.G., *Doctoral (Chem.) Dissertation,* Moscow, 1993.
21. Dunbar, I.H., Maclagan, R.G.A.R., and Parr, R.G., *J. Mol. Struct.,* 1974, vol. 23, no. 1, pp. 121–129.
22. Choudary, U.V., Gingerich, K.A., and Kingcade, J.E., *J. Less-Common Met.,* 1975, vol. 42, no. 2, pp. 111–126.
23. Kuligina, L.A. and Semenov, G.A., *Vestn. Leningr. Gos. Univ., Ser. Fiz., Khim.,* 1985, no. 18, pp. 39–45.
24. Lopatin, S.I., Semenov, G.A., Kirsanov, D.O., and Shugurov, S.M., *Zh. Obshch. Khim.,* 2000, vol. 70, no. 3, pp. 383–385.